ELECTRON TECHNOLOGY
ISSN 1897-2381
http://www.ite.waw.pl/etij/
Internet Journal

PHOTOELECTRIC MEASUREMENT METHODS AND THE UNIVERSAL MEASUREMENT SYSTEM FOR PRECISE PARAMETER DETERMINATION OF SEMICONDUCTOR STRUCTURES

P. MACHALICA[1], S. PORĘBSKI[1], J. ZAJĄC[1], L. BOROWICZ[1], A. KUDŁA[2], H.M. PRZEWŁOCKI[2]

[1]Industrial Institute of Electronics, ul. Długa 44/50, 00-241 Warszawa, Poland
[2]Institute of Electron Technology, Al. Lotników 32/46, 02-668 Warszawa, Poland

Received: September 19, 2002; published: December 31, 2002

ABSTRACT

In this article a new Multifunctional System for Photoelectric Measurements of Semiconductor Structures (MSPM) is presented. The system enables very accurate photocurrent measurements at levels as low as 10 fA. Measured structures can be biased by sequences of DC voltages and stimulated by light beams of predefined wavelengths and powers. The software controls all the system actions allowing flexibility in retrieving data stored in the related databases.

1. Introduction

Photoelectric measurement methods have been used to determine parameters of semiconductor materials and structures since the early days of the semiconductor era. A review of the earlier generation of these methods, as applied to determination of semiconductor structure parameters can be found in [1, 2].

In this article a brief description and examples will be given of the principles on which the new generation of photoelectric methods are based, and a new measurement system will be presented, which allows implementation of these methods.

The principles of the new measurement methods, as well as the new theory on which these methods are based have been developed in the Institute of Electron Technology (IET), while the measurement system has been designed, built and tested in the Industrial Institute of Electronics (IIE), in accordance with the requirements set by IET. The team of researchers and specialists (from IET, IIE and from the Warsaw University of Technology – WUT), who contributed significantly to the implementation of the measurement system has been awarded the title: "CHAMPION OF TECHNOLOGY – Warsaw 2001" and has received the first prize of the Polish Federation of Engineering Associations – NOT.

2. Photoelectric measurement methods

Photoelectric methods have been used to determine a wide range of properties of various semiconductor structures. Since the nineteen sixties, they proved to be particularly useful in determining important parameters of metal-oxide-semiconductor (MOS) and metal-insulator-metal (MIM) structures. These methods were often used to determine band structures of MOS and MIM systems, with particular emphasis on determination of barrier heights at the interfaces [3–6]. They were also used to determine charge distributions and to monitor charge trapping in the dielectric (see e.g. [5, 7, 8]). Photoelectric methods of this generation are still successfully used to determine band structures of MOS systems in which "new dielectrics" such as Al_2O_3 or ZrO_2 are applied [9, 10]. A comprehensive review of this generation of photoelectric methods is given in [11]. These methods were mostly based on the theory worked out by Fowler [12] and Kane [13], and further developed by Powell and Berglund [3–5, 14]. In this theory it is assumed that the electric field E in the dielectric is the driving force for the current flow, while other effects such as diffusion of carriers are considered to be negligible. Hence this theory and the measurement methods based on it are applicable only in cases when the electric field E is large enough.

Recently, a new theory of photoelectric phenomena in MOS (and MIM) structures has been developed [15–17], which allows prediction and interpretation of MOS structure characteristics in case when the electric field E in the dielectric is close to zero. Based on this theory, a new generation of MOS structure photoelectric measurement methods has been developed. In particular, it results from this theory that from photoelectric characteristics of a MOS structure, a gate voltage value $V_G = V_{G0}$ can be found, at which the voltage drop in the dielectric V_I is zero, as shown in Fig. 1. This V_{G0} value can be used to determine several basic parameters of MOS structures, as discussed below.

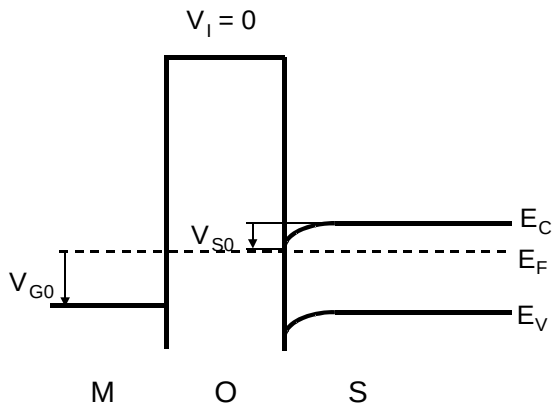

Fig. 1. Band diagram of the MOS structure for gate voltage $V_G = V_{G0}$.

The V_{G0} voltage can be determined from a set of photocurrent I vs. gate voltage V_G characteristics, such as the ones shown in Fig. 8. This can usually be done with the accuracy of the order of ± 1 mV. Once the V_{G0} value has been found, basic parameters of the MOS structure can be determined. Particularly accurate and effective is the method of determination of the effective contact potential difference (ECPD), called also the ϕ_{MS} factor. This results from the following.

The gate voltage V_G of the MOS structure is always given by a sum:

$$V_G = V_I + V_S + \phi_{MS} \tag{1}$$

where V_I is the voltage drop in the dielectric and V_S is the surface potential in semiconductor. Since $V_I = 0$ for $V_G = V_{G0}$, we have:

$$V_{G0} = V_{S0} + \phi_{MS} \tag{2}$$

where V_{S0} is the value of V_S for $V_G = V_{G0}$. Hence, from the measured V_{G0} value ϕ_{MS} can be determined if V_{S0} is known. The V_{S0} value can either be determined by standard methods from capacitance vs. voltage $C(V_G)$ characteristics (as the V_S value, which corresponds with capacitance C at $V_G = V_{G0}$), or it can be minimized, so that $V_{G0} \cong \phi_{MS}$ results from (2). This can be obtained for MOS structures with heavily doped substrates, in which case $V_{S0} < (5 \div 10)$ mV is readily achieved. The ϕ_{MS} measurement method described above has been fully verified and has been proved to be the most accurate and sensitive of the existing methods of this parameter determination [17, 18].

Other important parameters of MOS structures can also be determined using the photoelectric characteristics in the vicinity of the $V_G = V_{G0}$ point. For instance, for $V_G = V_{G0}$:

$$Q_{S0} = -Q_{eff} \tag{3}$$

where Q_{S0} is the semiconductor surface charge at $V_G = V_{G0}$ and Q_{eff} is the effective charge in the MOS structure. This property results from the fact that at $V_G = V_{G0}$ the electric field in the dielectric E is zero. Using Eq. (3), the value of Q_{eff} can be determined by finding (from standard $C(V)$ characteristics calculation methods) the V_{S0} value corresponding with V_{G0} and Q_{S0}.

It also results from the theory, that the slope of the $I(V_G)$ characteristics (such as the ones shown in Fig. 8) can be used as a measure of the trapping properties of the dielectric [17]. In particular, the relative changes of these trapping properties (as results from, e.g. plasma processing of MOS structures) can be precisely determined this way.

It is worthwhile to note here, that the zero voltage drop in the dielectric situation, taking place at $V_G = V_{G0}$ (see Fig. 1) is in a way analogous to the well known flat-band situation in the semiconductor, which takes place at the flat-band voltage $V_G = V_{FB}$. This flat-band voltage value V_{FB}, as determined from standard measurements of capacitance vs. voltage characteristics $C(V_G)$ is widely used to determine parameters of MOS structures. However, it is important to realize that it is very difficult to determine the V_{FB} value, with the accuracy better than ± 100 mV, while the accuracy of ± 10 mV is readily obtained in photoelectric measurement of the V_{G0} value (and usually it is considerably better). Consequently, photoelectric MOS structure measurement methods based on V_{G0} determination are in some cases much more accurate than electrical methods based on determination of V_{FB}.

3. The MSPM measurement system

The multifunctional system for photoelectric measurements of semiconductor structures (MSPM) integrates the following subsystems responsible for individual tasks: measurement subsystem (MS), optical subsystem (OS), positioning subsystem (PS), visual observation subsystem (VOS) and sub-subsystem for data acquisition, archiving and processing of measurement results (DAS). The pictorial diagram of the system is shown in Fig. 2.

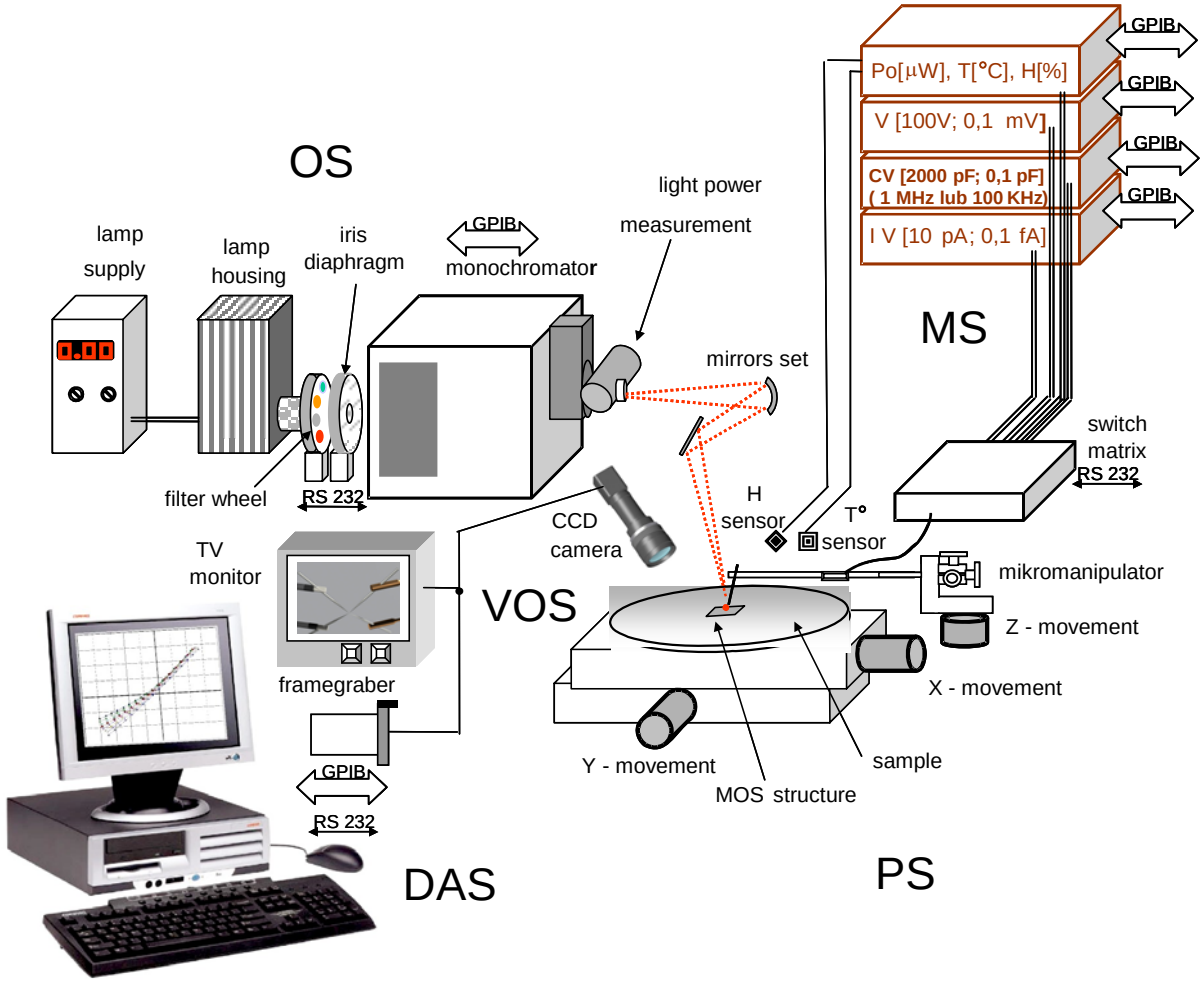

Fig. 2. The pictorial diagram of the multifunctional measurement system.

3.1. Measurement subsystem (MS)

The MS includes, top-class precision measurement tools and sources of bias voltages. Figure 3 presents the structure of the MS.

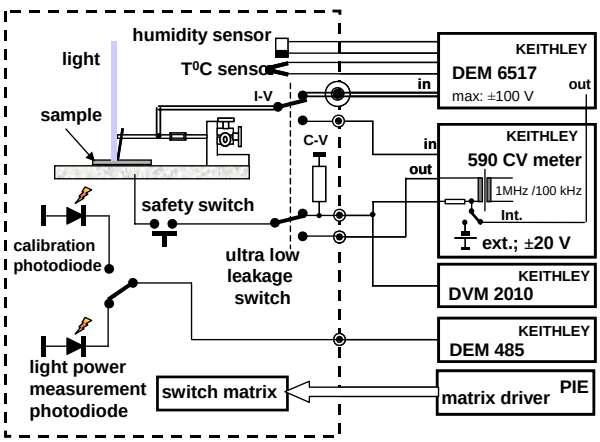

Fig. 3. Block diagram of the measurement subsystem.

The practically achievable measurement parameters, are listed below:

- dc voltages – up to ± 100 V with a resolution of 1 mV (for V_{G0} measurements),
- very small dc currents with a resolution of 1 fA (fA = 1E-15 A),
- capacitance (with a measurement signal of frequency f = 1 MHz or 100 KHz) – up to 2000 pF with a top resolution of 100 fF,
- temperature in the room temperature range with a resolution of 0.1°C,
- relative humidity from 0 to 100 % with a resolution of 1 %,
- light beam power from 0.01 up to 20 µW in the deep *UV* range.

A special automatic switch with insulation >1.0E15 Ω, which was not available on the market, had to be developed to allow measurements of very low photocurrents.

3.2. Optical subsystem (OS)

In photoelectric measurements, the MOS structure is illuminated with a light beam of software controlled wavelength and light power. The OS is responsible for that task and includes the following devices and subsystems:

- light source – xenon 150 W UV enhanced discharge lamp,
- lamp power supply with current and light power control loops,

- monochromator with software controlled selection of grating type, light wavelength and widths of input and output slits,
- iris diaphragm for the control of power of the light beam at the input slit of the mono-chromator,
- filter wheel with software controlled selection of filters for specified light wavelengths, to eliminate undesired spectrum ranges due to light diffraction on the diffraction grating,
- light power measurement set at the output of the monochromator, where part of light is directed to the photodiode. The signal from this photodiode is used for adjustment of the iris diaphragm, which allows control of the light power,
- set of mirrors for forming a light spot on the tested structure.

In Fig. 4 the block diagram of the optical subsystem is shown.

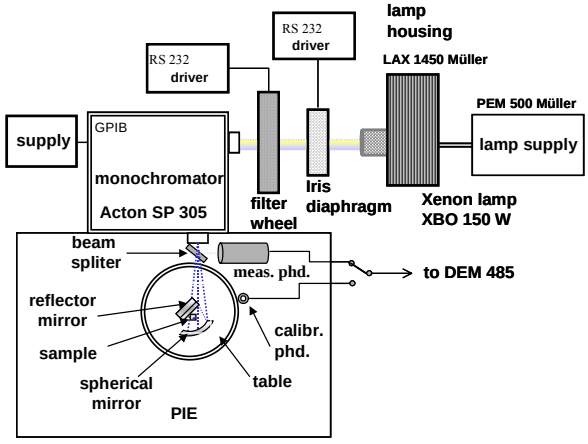

Fig. 4. Block diagram of the optical subsystem.

The light beam from the xenon discharge lamp passes through the condenser, iris diaphragm, and the filter wheel into the mono-chromator's input slit. The light beam going out of the monochromator with software controlled wavelength is split into two beams – one (10%) directed into the measurement set and the other one (90%) to the mirrors focusing light on the sample.

Light beam power that can be achieved for a selected wavelength on the tested structure is an important parameter characterizing the OS. A calibration photodiode is fixed on the testing table in a way ensuring that its active surface is on the table level. To assure that the power of the light beam focused on the measured structure is properly determined, correlation has been found between signals from the calibration photodiode and from the photodiode in the light power measurement set, which controls the iris diaphragm.

The parameters of the OS achieved in practice are:

- light source: xenon discharge lamp 150 W,
- range of light wavelengths: 190 nm to 700 nm, with 2 nm resolution,
- range of the light power on the testing table: from 0 to 20 μW in deep *UV*,
- light stability: 0.3 %.

3.3. Visual observation (VOS) and positioning (PS) subsystems

The PS allows positioning the tested structure in relation to the light beam and ensuring stable measurement contact. Electromagnetic interference shielding and elimination of the outside light is ensured during the measurements of the structure.

The tested wafer is vacuum fixed to the table. The measurement probe is attached to a platform with external regulation along the *Z* axis. This allows manipulating the probe within the observation field, when the cover of the PS is closed. Observation of the measured structure is assured by the VOS which includes a CCD camera, a TV monitor and a fibre optic illuminator. Figure 5 shows the configuration of the VOS.

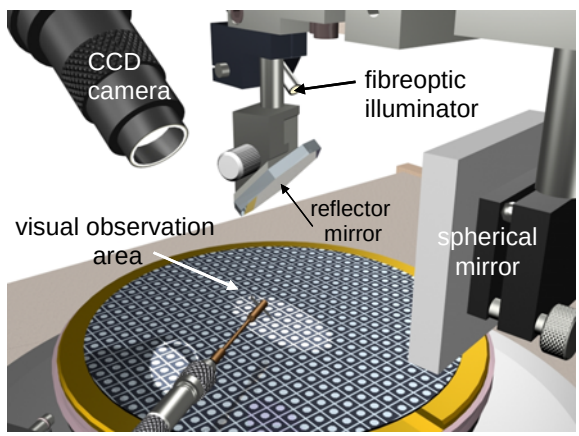

Fig. 5. Visual observation subsystem.

Light beam from the fibre optic subsystem is directed to the table via a spherical mirror. The measuring probe and its shadow are visible on the TV monitor. This allows to precisely lower the probe to the contacts of the measured structure without damaging them. The correct position of the probe is achieved when the probe tip touches the tip of the shadow on the TV screen .

The VOS allows also to precisely position measured structures in relation to the light beam, which is particularly important in case of small geometry structures.

The practically achieved parameters of the PS are:

- maximum diameter of semiconductor wafers with structures: 150 mm,
- positioning accuracy: ±20 μm,
- isolation of the measuring micromanipulator: > 1.0E15Ω,
- shielded and light-proof measurement chamber.

3.4. Data acquisition, processing and archiving subsystem (DAS)

The DAS consists of Pentium computer with GPIB and RS232 interfaces. Measurement devices are controlled by GPIB, while the monochromator, filters, diaphragm and switch matrix are controlled by RS232 ports. The system software is controlled by WINDOWS NT operating system.

Figure 6 presents a simplified block diagram of the system software.

The main measured values include the current of the structure I and its capacitance C. During the measurements the structure is activated with V bias voltage and light of a predefined wavelength λ and power P. Series of measured values are organised as families of characteristics with one of the values V, λ, P as independent variable, the other one as a family

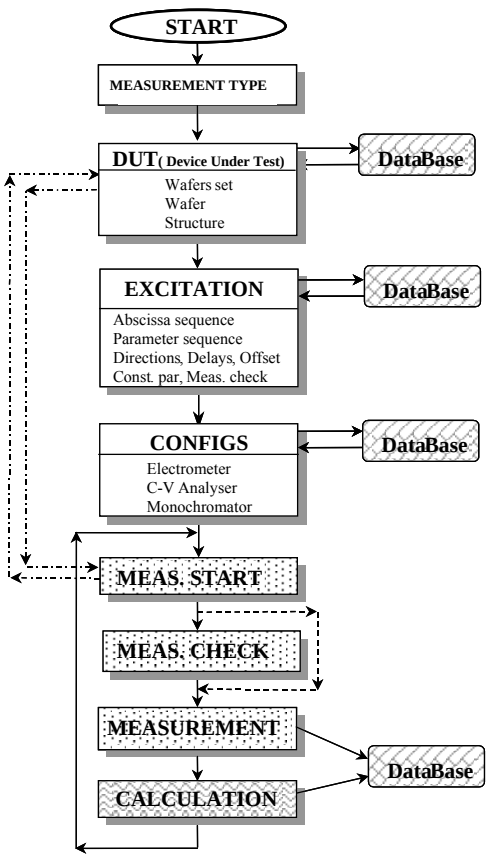

Fig. 6. The software block diagram.

parameter, while the remaining one is constant during the measurements for the whole family. The family can include a number of characteristics (branches) measured for the same value of the family parameter. E.g. the family $I(V)$: λ: Pc includes a number of curves representing the relationship between the current I and bias voltage V. Each curve is measured for a different wavelength λ, while the light power Pc is constant for the whole family.

The software can operate in two modes:

New measurements

Data review

In *New measurements* mode the software allows designing a measurement session by selecting parameters from the list or entering the values in subsequent windows.

In *Measurement object* window the following parameters are determined:

- type of the characteristic family (1 out of 10 types in 4 groups – $I(V)$, $I(\lambda)$, $C(V)$, $I(P)$),
- identifications, basic parameters and descriptions of the measured sample (at the levels of group, wafer and structure).

Then, in the *Input* window, the lists of values are determined as:

- a sequence of independent variables,
- a sequence of family parameters.

Monotonic sequence lists can be obtained from the database, or new lists can be created and recorded. Opening of the control procedure in *Prestart* window can be also programmed.

The *Configuration* window allows to configure:

- electrometer,
- C-V analyser,
- monochromator.

Configuration parameters can be drawn from the database or new configurations can be created and input into the database.

Depending on the decision, before the measurements start, the *Prestart* window can be opened, which allows to stimulate and check reaction of the tested sample and to set the meters to zero directly before the measurements, as well.

During the measurements, results are displayed in the *Measurements* window on a current basis as a chart or table. Major information on the tested sample and measurement conditions are displayed under the chart. Upon completion of measurements, processing of data can be started, yielding physical characteristics of the samples displayed as charts or tables in a special window. A set of calculated parameters and their presentation is connected with a characteristic family type. After completing measurements and processing, the user can repeat measurements without introducing any changes, change the tested object or design a new measurement session. The measurement session design, results and measurement conditions as well as calculation terms are recorded in the data bases.

4. Examples of measurement results

In this section examples are given of various types of characteristics taken using the MSPM, demonstrating the sensitivity, precision and reproducibility of the measurements.

In Fig. 7 an $I(V)$ characteristic is shown taken for a 1E12 Ω resistor by applying a sequence of voltages changing from –25 mV to 25 mV and back from 25 mV to –25 mV, in 5 mV steps. This characteristic

shows the excellent reproducibility of measurement results, as well as, good linearity of the characteristic even in the range of currents as low as just a few fA.

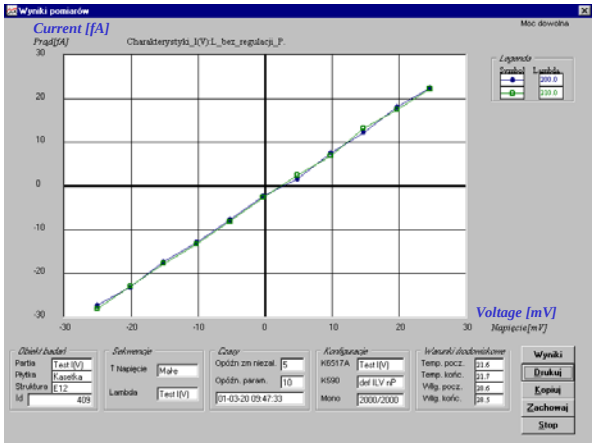

Fig. 7. *I*(*V*) characteristics taken for a 1E12 Ω resistor.

Figure 8 demonstrates a family of photocurrent *I* vs. gate voltage *V* characteristics of a MOS structure, taken for different wavelengths λ (230 ÷ 244 nm) of the *UV* light beam of constant power *P* illuminating the sample.As predicted by the theory [15–17], the *I(V)* characteristic which is symmetrical in respect to the $I = 0$ point intersects the voltage axis at $V = V_{G0}$, where V_{G0} is the gate voltage at which the voltage drop in the dielectric of the MOS structure is zero ($V_I = 0$).

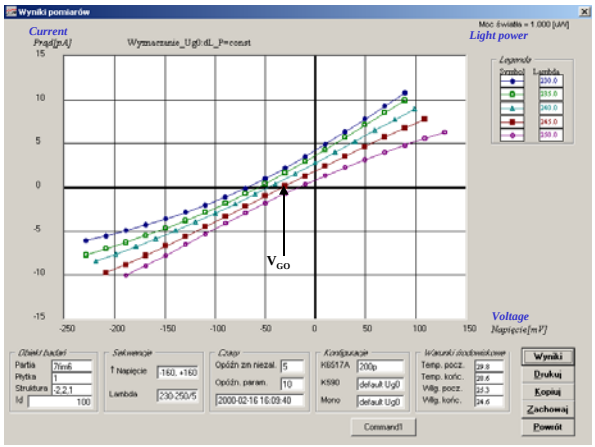

Fig. 8. Photocurrent *I* vs. gate voltage *V* characteristics of a MOS structure taken for different wavelengths λ of the *UV* radiation illuminating the structure. The value of the V_{G0} voltage is also marked.

The value of V_{G0} is used to determine important parameters of MOS structures, as described in [15–17].

In Fig. 9 a family of photocurrent *I* vs. wavelength λ characteristics are shown, taken for a range of different gate biases *V* (3, 6, 9 and 12 V) of a MOS structure. Such characteristics are widely used to determine potential barrier heights in MOS structures, as described in [6].

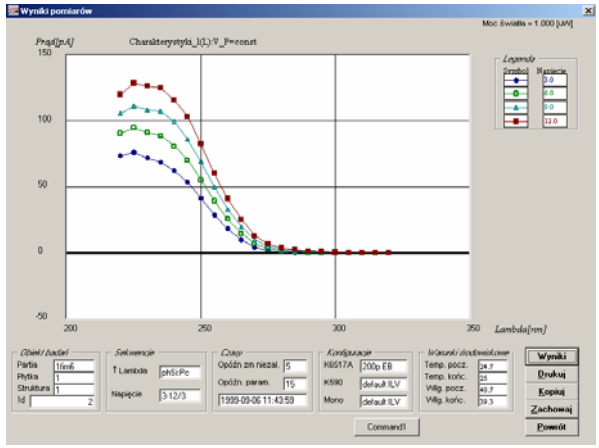

Fig. 9. Photocurrent *I* vs. wavelength λ characteristics of a MOS structure, taken for different gate biases *V*.

Figure 10 shows capacitance *C* vs. gate voltage *V* characteristics of a MOS structure, taken both in the darkness and under illumination by a light beam of wavelength $\lambda = 226$ nm and power $P = 3$ μW. Such *C*(*V*) characteristics are very useful in determining MOS structure parameters (see e.g. [9]).

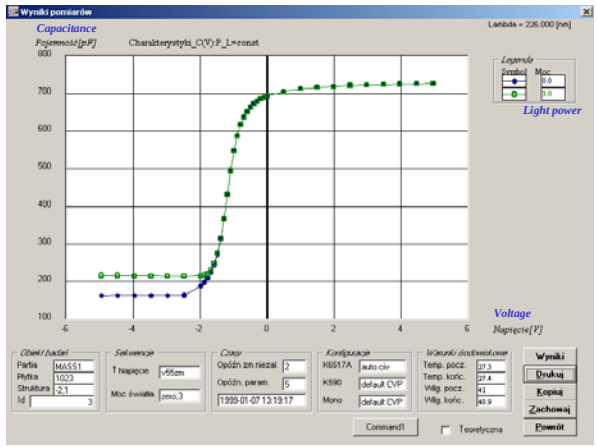

Fig. 10. Capacitance *C* vs. gate voltage *V* characteristics of a MOS structure, taken in the darkness and under illumination of the sample by a light beam of wave length $\lambda = 226$ nm and power $P = 3$ μW.

The MSM system allows determination of the barrier energy using Powell method [3], for internal photoemission both from metal to insulator and from semiconductor to insulator. Example of related characteristics are shown in Fig. 11.

Barrier energy, in this method, is determined in two steps: the photocurrent $I^{1/p} = f(V, V_{G0}, tox)$ characteristics are plotted for different photon energies (the *p* is a factor dependent on excited electron distribution), next the barrier energy and its field dependence shown in figure below are determined by extrapolation of $I^{1/p} = f(V, V_{G0}, tox)$ characteristics to zero current. Measurement of the photocurrent from single electrode is possible, because in the MOS structure, hole emission is small compared to electron emission.

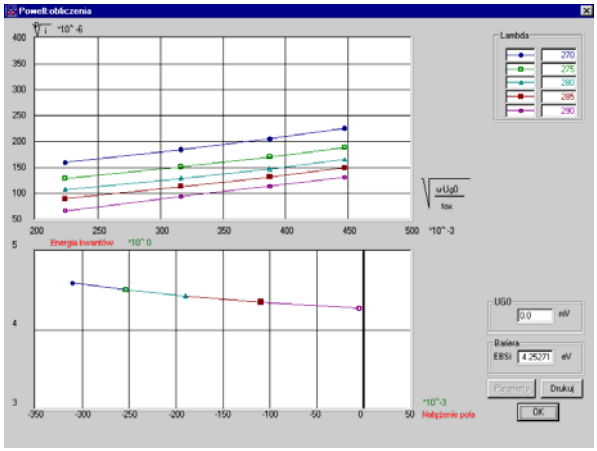

Fig. 11. Example of barrier energy determination for internal photoemission from Si to SiO_2.

Using measured $I(\lambda,V)$ characteristics barrier energy can be also determined using Fowler method as described in [6, 12, 14].

5. Summary

In this paper the MSPM system is described, which allows automated measurements to be made of various semiconductor structures complex characteristics. Advanced metrological parameters of the system, such as sensitivity, accuracy and stability of measurement results are demonstrated. The system is particularly useful for photoelectric measurements at low current levels of structures illuminated by deep *UV* radiation. Top quality measurement equipment produced by leading manufacturers is integrated into the system. The hardware and the related data bases are fully controlled by software, which allows archiving of measurement results, measurement conditions, data analysis results, etc. The MSPM has been successfully used during the last few years in the Institute of Electron Technology in Warsaw, for taking thousands of different characteristics of various structures sent for characterization from several leading scientific institutions in the world.

REFERENCES

1. E. H. NICOLLIAN, J. BREWS, *MOS Physics and Technology*. Wiley, New York, 1982.
2. D. K. SCHRODER, *Semiconductor Material and Device Characterization*, Wiley, New York, 1990.
3. R. J. POWELL, J. Appl. Phys., 1970, **41**, 2424.
4. C. N. BERGLUND, R. J., POWELL J. Appl. Phys., 1971, **42**, 573.
5. R. J. POWELL, C. N. BERGLUND, J. Appl. Phys., 1971, **42**, 4390.
6. A. KUDLA, Doctor's Thesis Institute of Electron Technology, Warszawa, 1997 (in Polish).
7. H. M. PRZEWLOCKI, J. Appl. Phys., 1985, **57**, 5359.
8. D. J. DIMARIA, J. Appl. Phys., 1976, **47**, 4073.
9. V. V AFANAS'EV, M. HOUSSA, A. STESMANS, M. M. HEYNS, Appl. Phys. Lett., 2001, **78**, 3073.
10. V. V. AFANAS'EV, M. HOUSSA, A. STESMANS, M. M. HEYNS, J. Appl. Phys., 2002, **91**, 3079.
11. V. K. ADAMCHUK, V. V. AFANAS'EV, Progr. Surf. Sci., 1992, **41**, 111.
12. R. H. FOWLER, Phys. Rev., 1931, **38**, 45.
13. E. O. KANE, Phys. Rev., 1962, **127**, 131.
14. R. J. POWELL, J. Appl. Phys., 1969, **40**, 5093.
15. H. M. PRZEWLOCKI, J. Appl. Phys., 1995, **78**, 2550.
16. H. M. PRZEWLOCKI, J. Appl. Phys., 1999, **85**, 6610.
17. H. M. PRZEWLOCKI, Solid-State Electron., 2001, **45**, 1241.
18. H. M. PRZEWLOCKI, Electron Technol., 1993, **26**, 3.